PG
Petroleum Geoscience

Research article

Published online December 18, 2014 doi:10.1144/petgeo2014-065 | Vol. 21 | 2015 | pp. 35–42

Creation of pre-oil-charging porosity by migration of source-rock-derived corrosive fluids through carbonate reservoirs: one-dimensional reactive mass transport modelling

Wolfgang van Berk[1*], Yunjiao Fu[2] & Hans-Martin Schulz[2]

[1] Clausthal University of Technology, Department of Hydrogeology, Leibnizstraße 10, D-38678 Clausthal-Zellerfeld, Germany
[2] Helmholtz Centre Potsdam – GFZ German Research Centre for Geosciences, Section 4.3 Organic Geochemistry, Telegrafenberg, D-14473 Potsdam, Germany
* Correspondence: wolfgang.van.berk@tu-clausthal.de

Abstract: Locally increased porosity of carbonate reservoir rocks may result from acidic fluids that migrated as a pre-oil phase through the reservoir. Here, hydrogeochemical modelling, which is based on the principles of chemical equilibrium thermodynamics, is performed to test such a hypothetical concept. Despite the generic nature of the model, the modelling results give basic and quantitative insights into the mechanisms of calcite dissolution in carbonate reservoirs induced by migrating acidic and corrosive aqueous fluids.

The hydrogeochemical batch modelling considers pre-oil-phase aqueous fluids that form by kerogen maturation in siliciclastic source rocks underlying the carbonate reservoir rocks. Although saturated with respect to calcite, migration of such fluids through the carbonate reservoir triggers continuous calcite dissolution along their migration path following a decreasing pressure and temperature regime. One-dimensional reactive transport modelling reveals that thermodynamically controlled chemical re-equilibration among pre-oil-phase fluids, calcite and $CO_{2(g)}$ is the driving force for continuous calcite dissolution along this migration path. This reflects the increasing solubility of calcite in the system 'pre-oil-phase fluids/calcite/$CO_{2(g)}$' with decreasing pressure and temperature. In consequence, such fluids can preserve their calcite-corrosive character, if they are exposed to continuously decreasing pressure and temperature along their migration path through the reservoir.

Supplementary material: The modelling input files to ensure retraceability of our modelling approach and its results are available at http://www.geolsoc.org.uk/SUP18802.

Received 10 September 2014; **revised** 30 October 2014; **accepted** 3 November 2014

The hypothetical process

Increased porosity of carbonate reservoir rocks may or may not be interpreted as a result of late diagenetic calcite dissolution caused by acidic fluids that migrated through the reservoir immediately before or during migration of the actual oil phase (see Lambert *et al*. 2006; Ehrenberg *et al*. 2012). Acidic components of such corrosive fluids (carbonic acid and carboxylic acids) can be generated during early kerogen maturation in source rocks (Barth & Bjørlykke 1993; Seewald 2003), but also by oil degradation (hydrolytic disproportionation: Helgeson *et al*. 1993; Pokrovskii & Helgeson 1994; Seewald 2003).

Acidic, corrosive and aqueous oil-/gas-bearing fluids (ACF) are generated within siliciclastic source rocks, and, subsequently, are expelled before and in front of a migrating oil-dominated phase. Once expelled, such ACF migrate from the source rock into and through the reservoir. The expelled fluids change their composition from initially water- and gas-dominated fluids to later oil-dominated fluids over the course of time. Along their migration path through carbonate reservoir rocks following a decreasing pressure and temperature regime, ACF can cause calcite dissolution and create secondary porosity due to their corrosive character, provided that the ACF are still undersaturated with respect to calcite when arriving at and migrating though the reservoir. The mass-action law constants for the equilibrium reactions between ACF, calcite and $CO_{2(g)}$ depend on temperature and pressure, and, therefore, change along this migration path. As a result, the overall effect of decreasing temperature and pressure on the equilibrium constants of all coupled reactions between aqueous, gaseous and solid species may lead to an increasing solubility of calcite, and, consequently, to continuous calcite dissolution along the migration path of ACF.

Motivation and aim

The development of a hydrogeochemical modelling approach presented in this contribution was encouraged by a hypothetical concept about dissolution of micritic calcite in Middle Eastern oil fields (Ehrenberg *et al*. 2012) and by the conclusions drawn by Ehrenberg *et al*. (2012). Ehrenberg *et al*. (2012, p. 227) stated that: (1) 'diagenetic reactions must be constrained geochemically'; and (2) that 'the theory that dissolution by acid pore water has produced significant net increases in bulk porosity has not been supported by models of mineral solubility and fluid flow'.

The hydrogeochemical, one-dimensional reactive mass transport (1DRT) modelling presented here aims to test whether such a hypothetical concept about porosity creation in carbonate reservoirs is tenable with regard to the thermodynamics of chemical equilibrium and the principles of reactive mass transport. Our modelling is of generic nature, and ignores any absolute spatial and temporal attributes of mass transport. Thus, the aim of this study is neither to reproduce reactive mass transport processes nor to predict their effects on the spatial and temporal distribution of calcite dissolution and corresponding porosity creation on a reservoir scale (e.g. Melville *et al*. 2004).

Such 1DRT calculations link 1D, purely advective porewater flow with the equilibrium thermodynamics of simultaneous chemical water–rock–gas interactions. Thereby, the presented modelling approach aims to test whether porosity creation by

Table 1. *Batch and one-dimensional reactive mass transport modelling scenarios*

Scenario	Geosystem	Aim	Model type	Equilibrium phases[a]	Amount of KMP[b]	Results presented
1	Source rock	ACF generation[a]	Batch	Qz, An, Ab, Kfs Kao, Cc, Gas	0.5–10	Figure 1
2	Source rock	ACF generation	Batch	Qz, An, Ab, Kfs Kao, Cc, Gas	0.1	*c*
3	Source rock	ACF generation	Batch	Qz, An, Ab, Kfs Kao, Cc, Gas	1.0	Supplementary material
4	Source rock	ACF generation	Batch	Qz, An, Ab, Kfs Kao, Cc, Gas	10.0	*c*
5	Source rock	Calcite saturation	Batch	Cc, Gas	0.1	Table 2
6	Source rock	Calcite saturation	Batch	Cc, Gas	1.0	Table 2
7	Source rock	Calcite saturation	Batch	Cc, Gas	10.0	Table 2
8	305 atm/85 °C	Solubility of calcite	Batch	Cc (pCO_2 = 10 atm)[d]	none	Table 3
9	205 atm/55 °C	Solubility of calcite	Batch	Cc (pCO_2 = 10 atm)[d]	none	Table 3
10	Reservoir rock	Calcite dissolution during migration	1DRT[e]	Cc, Gas	0.1	Figure 4a
11	Reservoir rock	Calcite dissolution during migration	1DRT	Cc, Gas	1.0	Figure 4b
12	Reservoir rock	Calcite dissolution during migration	1DRT	Cc, Gas	10.0	Figure 4c

[a]Qz, Quartz; An, Anorthite; Ab, Albite; Kfs, K-feldspar; Kao, Kaolinite; Cc, Calcite; Gas, multicomponent gas ($CH_{4(g)}$, $CO_{2(g)}$, $H_{2(g)}$) potentially formed at a fixed pressure of 305 atm.
[b]Stepwise addition of kerogen maturation products with given amounts (KMP; simplified by CH_4, CO_2, H_2, and acetic acid).
[c]No detailed results.
[d]Carbon dioxide partial pressure.
[e]One-dimensional reactive transport modelling.

pre-oil-charging in principle can result from long-term migration of source-rock-derived corrosive aqueous fluids through carbonate reservoirs under predefined conditions. If so, the modelling results aim to give basic and quantitative insights into the reasons and mechanisms for potential in-reservoir calcite dissolution induced by migrating ACF. The modelling results may stimulate the geological discussion about this issue (see Lambert *et al*. 2006; Ehrenberg *et al*. 2012) with quantitative, plausible and verifiable arguments.

In addition to this 1DRT modelling, hydrogeochemical '0D' batch modelling was performed in order: (1) to reproduce the compositional evolution of aqueous fluids (ACF) driven by the chemical products of kerogen maturation in siliciclastic source rocks; and (2) to calculate and evaluate the effects of pressure and temperature conditions on the solubility equilibration between calcite, coexisting ACF-dominated aqueous solutions and CO_2-bearing gas.

We are aware that many issues related to flow and reactive mass transport in fractured, porous media (e.g. carbonate reservoir rocks) still 'remain at the frontier of research' (Berkowitz 2002; p. 878). Among other transport phenomena, reservoir rock dispersivity is a factor that needs an adequate characterization based on field data. Because of their generic nature, our 1DRT models consider simple and well-defined initial and boundary conditions for advective and reactive transport. These assumed conditions and parameter values may not reflect geological reality since quantitative data are unavailable. Nevertheless, several controlling factors remain unconsidered by our modelling: (1) the effects of calcite dissolution kinetics; (2) different types of porosity and carbonate minerals, such as high- and low-Mg-calcite, aragonite or dolomite instead of pure calcite ($CaCO_{3(s)} = Ca^{2+} + CO_3^{2-}$: $K^{a}_{s/calc}$); (3) different types of fractured and porous carbonate rock matrices; and (4) predefined temperature–pressure gradients differing from those applied by our modelling.

Conceptual models and modelling scenarios

Hydrogeochemical modelling of processes in source rocks

Generation of aqueous gas-bearing fluids with acidic and corrosive character (ACF)

Detailed field data about the composition of ACF in source rocks that are exposed to early kerogen maturation are lacking. Therefore, our modelling approach starts with one simple hydrogeochemical '0D' batch model (Table 1) and calculates the generic composition of ACF produced within the source rock. In addition, this batch modelling aims to conceptually reproduce the chemical interactions between the early products of kerogen maturation (KMP), an aqueous, sodium chloride-dominated solution and a generic siliciclastic source rock. These chemical interactions, which are driven by the release of KMP, lead to the formation of thermodynamically defined generic ACF compositions. Conceptually, the products of early kerogen maturation and also of oil degradation control the release of CH_4, CO_2, H_2 and carbonic acids (Seewald 2003). Therefore, and for the sake of simplicity, kerogen maturation is simulated by adding its products CH_4, CO_2, H_2 and acetic acid into the batch modelling reactor. In this study, their initial relative production ratios are set to 1.9 (for CO_2), 0.9 (for CH_4), 5.0 (for H_2) and 0.1 (for acetic acid: Seewald 2003; Helgeson *et al*. 2009; van Berk *et al*. 2009); molecular hydrogen and carbon dioxide will subsequently react to form additional methane. The initial ratio of CO_2 to acetic acid follows the findings of Barth & Bjørlykke (1993). These authors performed hydrous pyrolysis experiments (280–350 °C) and found that carbon dioxide dominates over organic acids (dominantly acetic acid) as acidic products (see also Helgeson *et al*. 1993). Under the predefined conditions in the '0D' batch model reactor characterizing source-rock conditions (305 atm/85 °C), these KMP dissolve in 1 l of a 1 molal (1 *m*) NaCl aqueous solution and drive reactions between the mineral phase assemblage (0.48 mol each of quartz and kaolinite; 0.01 mol each of calcite, anorthite, albite and K-feldspar) and an assumed potentially co-existing multicomponent gas ($CH_{4(g)}$, $CO_{2(g)}$ and $H_{2(g)}$) at a fixed total pressure of 305 atm (*c*. 3000 m depth under assumed hydrostatic pressure conditions). This multicomponent gas may form at saturation. Up to 10 mol of KMP are added to the aqueous solution in portions of 0.5 mol each. Based on the chemical thermodynamics of aqueous equilibrium reactions, the equilibrium species distribution and the mass conversion resulting from these interactions are calculated.

ACF saturation with respect to calcite and calculating ACF influx composition

The composition of ACF migrating into the carbonate reservoir rocks depends on the mass conversion of early kerogen maturation

Table 2. *Modelling results from batch modelling scenarios '5', '6' and '7'*

Scenario	KMP[a]	pH	cCa^{2+}_{total} (mmol kgw^{-1})	$cCO_{2(aq)}$ [b] (mmol kgw^{-1})	$cC(+IV)_{(total)}$ [c] (mmol kgw^{-1})	cCH_3COOH (mmol kgw^{-1})
5	0.1	5.30	105.3	27.7	36.6	0.7
6	1.0	4.90	142.2	177.9	200.2	16.0
7	10.0	4.72	337.8	429.3	462.6	174.4

[a]KMP: kerogen maturation products dissolved in ACF (mol kgw^{-1}).
[b]Total dissolved carbon dioxide
[c]Total dissolved carbonate carbon.

reflected by the amount of KMP in our batch model reactor. Such real compositional data are unavailable. To overcome this gap, sensitivity analyses were carried out by applying a broad range of KMP values in various modelling scenarios. Therefore, three similar scenarios ('2', '3' and '4': Table 1) were additionally performed to calculate the composition of ACF expelled from source-rock batch reactors that are exposed to 0.1, 1.0, and 10.0 mol of KMP, respectively.

The compositional data of the aqueous solutions calculated by these ACF-generation scenarios '2'–'4' were used as input data to calculate the equilibrium species distribution and the mass conversion in three additional batch reactors (scenarios '5'–'7'). The only mineral being initially present in these batch reactors is calcite; quartz and kaolinite are potential secondary minerals that may form at saturation. The rationale is meant to accomplish that the ACF produced by the release of the products of kerogen maturation will equilibrate with calcite (plus potentially formed kaolinite and/or quartz), and a potentially formed multicomponent gas ($CH_{4(g)}$, $CO_{2(g)}$ and $H_{2(g)}$) at 305 atm/85 °C, before migrating into and through the carbonate reservoir rock. Such equilibration leads to the formation of ACF, which are saturated with respect to calcite (Saturation Index ($SI_{calcite}$) = 0). Table 2 presents the chemical composition of such ACF, which: (1) are exposed to various amounts of KMP; and (2) subsequently achieved their saturation with respect to calcite (scenarios '5'–'7').

Hydrogeochemical modelling of in-reservoir processes

Batch modelling: effects of pressure–temperature on the equilibrium constant of calcite and on the solubility of calcite in the 'ACF–calcite–$CO_{2(g)}$' system

According to the hypothetical process (see the earlier section on 'The hypothetical process'), ACF migration through carbonate reservoir rocks proceeds along a decreasing pressure and temperature regime, and calcite may display a solubility that increases with decreasing pressure and temperature conditions. Two simple batch modelling scenarios ('8' and '9: Table 1) are performed to compare the effects of various pressure–temperature combinations (305 atm/85 °C v. 205 atm/55 °C) on calcite solubility in aqueous 1.0 m NaCl solutions. Both scenarios are calculated for the same pre-assigned $pCO_{2(g)}$ of 10 atm. In addition, the equilibrium constants for calcite dissolution ($CaCO_{3(s)} = Ca^{2+} + CO_3^{2-}$: K_s^a, in mol kgw^{-1} (mol per kg water)) are calculated for various pressure and temperature conditions.

One-dimensional reactive transport modelling: ACF migration through a calcite column

To investigate the effects of ACF migration on calcite dissolution along the migration path through the carbonate reservoir rock column, the 1D reactive mass transport modelling approach considers a 1D flow tube with an influx of ACF, which has achieved calcite saturation before the ACF enters the carbonate reservoir rock. Owing to the lack of field data about the ACF composition, three different generic ACF compositions (calculated in scenarios '5'–'7': results in Table 2) are used in the 1DRT modelling (scenarios '10'–'12': Table 1).

The 1D model of reactive ACF transport through the carbonate reservoir rock column considers advection as the only active hydraulic mass transport process that is coupled to simultaneous water–rock–gas interactions. Neither explicit definition of spatial (e.g. cell length) nor of temporal attributes (e.g. time step length, flow velocity) have been assigned to the cells of this 1D flow tube model. This also holds true for hydraulic parameters (e.g. hydraulic head gradient, permeability, porosity). Such a simple generic modelling approach aims to give basic and quantitative insights into the reasons and mechanisms for potential in-reservoir calcite dissolution induced by migrating ACF. In total, 10 cells (cell pore volume of 1.0 l; porosity of 10%) represent the ACF migration path through the carbonate reservoir rock column of undefined length. Advection is characterized by the 'number of pore volumes displaced' (n), which indicates how often the whole pore volume of the rock column has been displaced by the volume of ACF influx. During each time step, the inflowing ACF completely displaces the solution that filled the pore volume of the cells before. Subsequently, the chemical re-equilibration between the 'new' pore-filling solution, the mineral assemblage and the gas alters the composition of the system. Such 1DRT modelling scenarios consider a steady-state flow condition, corresponding mass fluxes, as well as a constant initial composition of the ACF influx in a generic carbonate reservoir.

A predefined P–T gradient extends over this 10-cell migration path ranging from 295 atm/82 °C (first cell: cell with ACF influx generated at 305 atm/85 °C) over 285 atm/79 °C, then 275 atm/76 °C and, finally, to 205 atm/55 °C in the last cell. This gradient generically represents a regional geothermal gradient of 0.03 °C m^{-1} of depth (equivalent to c. 0.1 atm of total pressure) under hydrostatic conditions.

Prior to the influx of ACF, 1.0 l of pore water fills each cell. For the sake of simplicity, this pore water is a 1 m NaCl solution, which is saturated with respect to calcite under the corresponding temperature and pressure conditions. Each cell of the reservoir rock model exclusively consists of pure calcite: 100 mol $CaCO_{3(s)}$ (equivalent to 10 009 g), which is sufficient to ensure the equilibration of inflowing ACF with calcite ($SI_{calcite}$ = 0), even at the highest 'number of pore volumes displaced' (n = 1000). Calcite is the only primary mineral before ACF influx; quartz and kaolinite are potentially secondary minerals. In addition, a potential multicomponent gas ($CH_{4(g)}$, $CO_{2(g)}$ and $H_{2(g)}$) may form, and co-exist with the mineral assemblage and the corresponding solution after equilibration under the specified pressure and temperature conditions along the flow path.

Modelling tools

The United States Geological Survey's Phreeqc Interactive 3.1.4-8929 computer code (Parkhurst & Appelo 2013) is our modelling tool for the batch and the 1DRT models. Based on the chemical thermodynamics of aqueous equilibrium reactions, this tool enables us to calculate the equilibrium species distribution, mass conversion and coupled 1D-advective mass transport. In combination with its

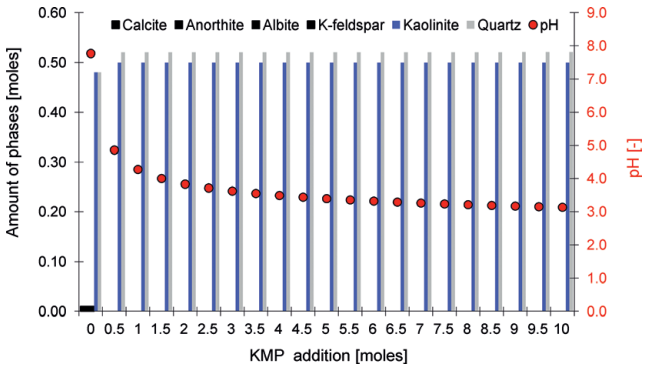

Fig. 1. Modelling results from batch modelling scenario '1'. ACF generation within siliciclastic source rocks: pH and mineral content depend on the continuous addition of kerogen maturation products (KMP). KMP addition of more than 0.5 mol leads to the complete consumption of the initial acid-buffering capacity by calcite, anorthite, albite and K-feldspar within the source rock (0.01 mol each; black bar).

phreeqc.dat database (Parkhurst & Appelo 2013), Phreeqc Interactive 3.1.4-8929 considers both the temperature and the pressure dependence of the mass-action law constants for the equilibrium reactions of involved aqueous, gaseous and solid species – with the exception of all acetate-bearing species and a few aqueous aluminium- and silicon-bearing species. The acetate species and their corresponding equilibrium constants are taken from the minteq.v4.dat database of Phreeqc Interactive 3.1.4-8929 and additionally defined in the input files.

Modelling results

Source-rock batch modelling

Generation of aqueous gas-bearing fluids with acidic and corrosive character (ACF)

The amount of organic carbon converted (e.g. in moles) to CO_2, CH_4 and CH_3COOH, and released by kerogen maturation, controls the acidity (pH, CO_2 and CH_3COOH) produced in the source rock. At high levels of such mass conversion of organic carbon, the release of this kerogen-derived acidity causes the total consumption of the acid-neutralization capacity in a siliciclastic source rock (Fig. 1). This capacity is initially provided by minor amounts of calcite, anorthite, albite and K-feldspar. Equilibration between the 1 m NaCl solution and the initial mineral assemblage – without any addition of KMP (scenario '1': Fig. 1) – leads to a pH of 7.8. The addition of 0.5 mol KMP completely dissolves calcite, anorthite, albite and K-feldspar due to acid attack; the corresponding pH decreases to 4.9 (Fig. 1). Feldspar dissolution drives the formation of secondary kaolinite and quartz. Owing to ongoing addition of KMP, kaolinite takes over the buffering of acidity. Slightly decreasing amounts of kaolinite and slightly increasing amounts of quartz characterize this stage of KMP addition. In parallel, resulting acidic solutions may have pH values as low as 3.1, and high concentrations of dissolved $CO_{2(aq)}$ (0.28 mol kgw^{-1} at maximum) and acetic $acid_{(aq)}$ (0.65 mol kgw^{-1}: equivalent to *c.* 39 g kgw^{-1} at maximum). These solutions co-exist: (1) with a strongly altered mineral assemblage within the source rock; and (2) with a gas that is dominated by methane and carbon dioxide at 85 °C and 305 atm. Under these conditions, extremely low oxygen fugacities ($\log fO_{2(g)}$) prevail in the range of −57.7 to −57.6.

ACF saturation with respect to calcite and calculation of ACF influx composition

Scenarios '5'–'7' can calculate the composition of ACF that are saturated with respect to calcite ($SI_{calcite}=0$). Conceptually, such aqueous solutions represent ACF that have achieved their calcite saturation along their *P–T* migration path before they enter the carbonate reservoir rock. Table 2 presents the compositional data of three different ACF that formed by the addition of increasing amounts of KMP (0.1, 1.0 and 10 mol kgw^{-1}: scenarios '5', '6' and '7') and which subsequently reached their calcite saturation. Such ACF show pH values ranging from 5.3 to 4.7, and they are characterized by high concentrations of calcium and carbonate carbon.

The solubility constant of calcite along a potential pressure–temperature gradient

Changes in pressure and temperature affect the equilibrium constants, K^a, of mass-action laws of minerals, aqueous species and gases. The migration of ACF through the carbonate reservoir rocks should be accompanied by a decrease in pressure and temperature. Therefore, the solubility equilibrium of calcite ($CaCO_{3(s)}=Ca^{2+}+CO_3^{2-}$: $K^a_{s/calcite}$) and of carbon dioxide gas ($CO_{2(g)}=CO_{2(aq)}$: K^a_H), representing only two reactions in a complex web of interacting reactions, change along the migration path of the ACF. Figure 2 presents the solubility constants for calcite calculated for various pressure–temperature conditions along a potential *P–T*–depth migration path of ACF through the generic carbonate reservoir rock. The results clearly indicate that the solubility constant for calcite increases with decreasing pressure–temperature conditions along such a migration path, by a factor of around 1.7 within the *P–T* range of 295 atm/82 °C–205 atm/55 °C.

The solubility of calcite in the system '1.0 m NaCl solution/calcite/$pCO_{2(g)}$' at various pressure–temperature combinations

Although the pressure and temperature dependence of the solubility constant of calcite (Fig. 2) is obviously of great relevance for calcite dissolution, the equilibrium constants of all other interconnected equilibrium reactions in the system 'ACF–calcite–$pCO_{2(g)}$' exert additional influence. To evaluate the overall effect of decreasing pressure and temperature on the solubility of calcite, its solubility (mmol kgw^{-1}) in aqueous, 1 m NaCl solutions that are exposed to the same $pCO_{2(g)}$ of 10 atm are calculated for two different pressure–temperature combinations (305 atm/85 °C and 205 atm/55 °C). Table 3 compares these pressure–temperature effects, and highlights that significantly greater amounts of both calcite and $CO_{2(g)}$ dissolved at 205 atm/55 °C until calcite saturation (23.8 mmol kgw^{-1} calcite) when compared to the amounts of dissolved calcite at 305 atm/85 °C (15.4 mmol kgw^{-1} calcite).

Modelling of 1D reactive mass transport in the reservoir

Scenarios '10'–'12' are performed to calculate the combined effects of: (1) the increasing solubility of calcite in the system '1.0 m NaCl solution–calcite–$pCO_{2(g)}$' with decreasing pressure and temperature conditions (Table 3; Fig. 2); and (2) the advective mass transport on the amount of calcite that dissolves along an ACF migration path from high- to low-pressure and -temperature conditions. Figure 3 presents the amounts of dissolved calcite and the corresponding equilibrium–pH values for scenario '11'. This scenario considers the average intensity of ACF generation by the release of 1.0 mol KMP (0.1 and 10.0 mol in scenarios '10' and '12', respectively) and subsequent saturation of ACF with regard to calcite ($SI_{calcite}=0$) in the source rock at 305 atm/85 °C, immediately before these equilibrated ACF enter the reservoir rock and trigger following re-equilibration at 295 atm/82 °C within the reservoir. In addition, the greatest 'number of pore volumes displaced' ($n=1000$) is considered. This number indicates how often the whole pore volume of the rock column has been displaced by the ACF influx.

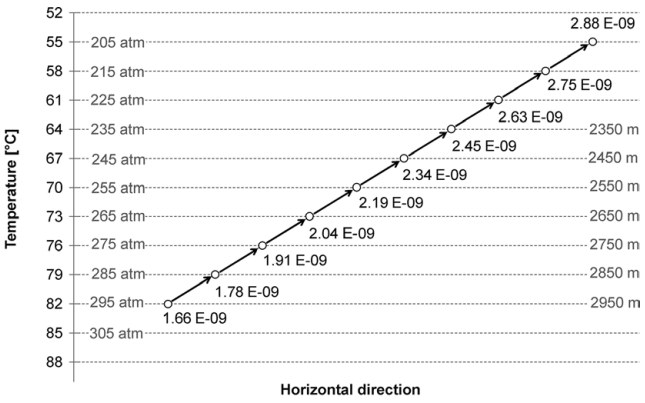

Fig. 2. Solubility constants for calcite ($CaCO_{3(s)}=Ca^{2+}+CO_3^{2-}$: K_s^a, in mol kgw^{-1}) calculated for various pressure and temperature conditions using the Phreeqc Interactive 3.1.4-8929 computer code in combination with its phreeqc.dat database (Parkhurst & Appelo 2013). Circles indicate the *P–T* conditions.

Although saturated with respect to calcite (at 305 atm/85 °C: before entering the carbonate rock column), ACF reaching the carbonate rock column at 295 atm/82 °C drive the continuous dissolution of calcite along the modelled *P–T* migration path – within all 10 cells of the 1DRT model (Fig. 3). Although the amount of dissolved calcite reaches its maximum within the first cell (3295 g cell^{-1}), the ACF leaving the first cell and filling the second cell drive calcite dissolution and consume 506 g calcite within the second cell at 285 atm/79 °C. Further ACF migration into higher levels of the reservoir at lower pressure and temperature conditions (e.g. 275 atm/76 °C) causes ongoing calcite dissolution along the migration path (Fig. 3).

While the ACF influx in scenario '11' has a pH of 4.90 (Table 2: scenario '6'), the ACF flux through the carbonate column is characterized by a slightly increasing pH up to 4.95 and finally up to 5.07 in the last cell along the *P–T* migration path. Here, 593 g of calcite are lost due to calcite dissolution (Fig. 3).

Figure 4 compares the modelling results from the 1DRT modelling scenario '11' with the results from '10' and '12', which consider a lower and a higher uptake of KMP into the ACF, respectively. The modelling results are presented in terms of the amounts of dissolved calcite along the ACF migration path when considering three different 'numbers of pore volumes displaced' ($n=10$, 100 and 1000, respectively: indicating how often the whole pore volume of the rock column has been displaced by the ACF influx). A comparison of the results presented in Figure 4 indicates that the migration of ACF triggers continuous calcite dissolution along the *P–T* gradient in all three 1DRT modelling scenarios, '10'–'12'. The level of calcite dissolution along the migration path depends on: (1) the uptake of KMP (0.1, 1.0 or 10.0 mol KMP) into the ACF (in other words, on the intensity of ACF formation in the source rock); (2) the duration of ACF influx ($n=10$, 100 or 1000: indicating how often the whole pore volume of the rock column has been displaced by the ACF influx); and (3) the pressure and temperature conditions along the migration path. A higher KMP content and longer periods of ACF influx (indicated by higher values of n) induce stronger calcite dissolution at *P–T* conditions ranging from 295 to 205 atm and from corresponding 82 to 55 °C.

Discussion of modelling results

ACF generation

Detailed hydrogeochemical field data about the ACF composition in source rocks are lacking. However, to conceptually reproduce the compositional development of ACF, our generic batch modelling is based on interactions between (1) acidity, (2) reducing agents, (3) aqueous solutions, (4) siliciclastic source rocks mineral assemblages and (5) a co-existing multicomponent gas under predefined temperature and pressure conditions (85 °C and 305 atm in the model). Our batch models consider kerogen maturation as the source for generated acidic and reducing components (CO_2, CH_3COOH, CH_4 and H_2) that are released into aqueous solutions. A degradation of oil already generated in the source rock, which would serve as an additional source for these chemical components, is not considered in our modelling.

Depending on the moles of organic carbon converted to CO_2, CH_4 and CH_3COOH (mass conversion of kerogen maturation), high aqueous concentrations of such organic carbon-derived carbon species (H_2 reacts with CO_2 to form additional CH_4) characterize the modelled aqueous solutions prevailing in source rocks. The gas co-existing with such aqueous solutions is characterized by low oxygen fugacities ($\log fO_{2(g)}$) ranging from −57.7 to −57.6 at 85 °C and 305 bar. These results from the batch modelling approach resemble the $\log fO_{2(g)}$ values calculated by Pokrovskii & Helgeson (1994), and reflect the thermodynamic constraints on the generation and maturation of petroleum in sedimentary basins in terms of redox transfer reactions (Helgeson *et al*. 1999).

Under these conditions, continuous KMP addition (CO_2, CH_3COOH, CH_4 and H_2: released during early kerogen maturation) can lead to a total consumption of the acid-neutralization capacity of the source rock, which is initially provided by minor amounts of calcite, anorthite, albite and K-feldspar. Kaolinite and quartz form at the expense of the feldspars within the batch model reactor simulating the source rock (Fig. 1). These modelled processes agree with the observation that carbon dioxide and acetic acid as the main acidic components of oil reservoirs can induce intense plagioclase dissolution and concurrent formation of kaolinite (e.g. in the Gullfaks oil field: Smith & Ehrenberg 1989; Ehrenberg & Jakobsen 2001). Hydrogeochemical modelling by van Berk *et al*. (2009, 2013) quantitatively reproduced this proven alteration of mineral assemblages in the Gullfaks field, which was driven by the products of oil degradation (CO_2, CH_3COOH and CH_4).

In addition to the equilibration with quartz and kaolinite, the acidic aqueous fluids generated in the batch model also achieve the state of saturation with respect to methane and carbon dioxide gas. These gases (and also hydrogen gas) coexist with these acidic aqueous solutions. High partial pressures of $CH_{4(g)}$ (237 bar) and $CO_{2(g)}$ (68 bar) characterize the composition of the co-existing gas, while the partial pressure of $H_{2(g)}$ (*c*. 10^{-5} bar) is minor, even after the addition of 10 mol of KMP. Consequently, the ACF show a high concentration of dissolved $CH_{4(aq)}$ (0.1 mol kgw^{-1}: 10 mol KMP addition). Dissolved $CO_{2(aq)}$ (0.3 mol kgw^{-1}) and acetic acid (0.65 mol kgw^{-1}; equivalent to *c*. 39 g kgw^{-1}) cause a low pH of about 3.1 and, correspondingly, a high acidity of the ACF at the maximum KMP addition of 10 mol (Fig. 1). This modelled ACF composition with high acetic acid/acetate concentrations (*c*. 39 g kgw^{-1} at maximum) is similar to the high organic acid

Table 3. *Modelling results from batch modelling scenarios '8' and '9'. Amount of dissolved calcite, dissolved $CO_{2(g)}$ and pH; equilibration with calcite and $pCO_{2(g)}$ of 10 atm at 305 atm/85 °C v. 205 atm/55 °C*

Scenario	Pressure–temperature (atm/°C)	Dissolved calcite (mmol kgw^{-1})	Dissolved $CO_{2(g)}$ (mol kgw^{-1})	pH
8	305/85	15.4	88.1	5.52
9	205/55	23.8	136.9	5.47

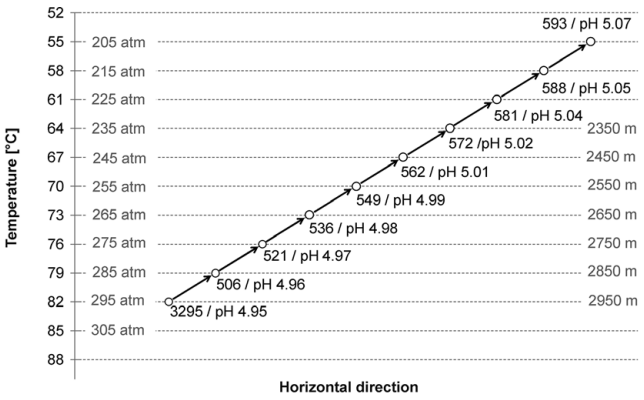

Fig. 3. Modelling results from 1DRT modelling scenario '11'. Amount of dissolved calcite (g cell^{-1}: first number next to the circles) and corresponding pH values along the migration path of ACF through the carbonate reservoir rock column. 'Number of pore volumes displaced': $n = 1000$. For the corresponding ACF influx composition see Table 2 (scenario '6'). Circles indicate the *P–T* conditions.

concentrations measured in oil field brines (*c*. 10 g kgw^{-1} at maximum: Seewald 2003). Such high organic acid concentrations in oil field brines are the result of recent–subrecent oil degradation. Consequently, even higher concentrations could be expected in ACF-bearing brines that are generated by kerogen maturation and subsequent oil degradation already in the source rock.

In summary, organic–inorganic interactions are driven by the products of kerogen maturation and subsequent oil degradation already in siliciclastic source and reservoir rocks (Smith & Ehrenberg 1989; Ehrenberg & Jakobsen 2001; van Berk *et al*. 2009, 2013). Such organic–inorganic interactions represent the inevitable consequences of chemical thermodynamics of such systems under elevated temperature and pressure conditions; the involved hydrogeochemical reactions tend to reach (metastable) equilibrium conditions (Helgeson *et al*. 1993). The fit of the observations (Ehrenberg & Jakobsen 2001) and corresponding modelling results (van Berk *et al*. 2013), regarding such organic–inorganic interactions in reservoir rocks, indicate that our generic batch modelling of ACF generation provides rough, but plausible, estimates to characterize the composition of ACF expelled from siliciclastic source rocks.

Calcite dissolution and porosity creation triggered by the migration of ACF

Calculations of calcite solubility under different temperature and pressure conditions reveal an increase in calcite solubility in the system 'ACF–calcite–$CO_{2(g)}$' with decreasing temperature and pressure. This results from the pressure and temperature dependence of equilibrium constants, K^a, of mass-action laws involved in all interacting equilibrium reactions. Although significant, the solubility equilibrium reactions of calcite ($CaCO_{3(s)} = Ca^{2+} + CO_3^{2-}$: $K^a_{s/calcite}$) and carbon dioxide gas ($CO_{2(g)} = CO_{2(aq)}$: K^a_H) represent only two reactions in a complex web of more interacting reactions.

ACF migrate along a gradient of decreasing pressure and temperature. Before entering the carbonate reservoir or at the point of entry into the carbonate reservoir rock, ACF will saturate with respect to calcite (at 305 atm and 85 °C in our model). Then, ACF further migrate into and through the reservoir reaching areas that are characterized by lower temperature and pressure conditions (e.g. 295 atm and 82 °C). Such a change in temperature and pressure causes undersaturation of ACF with respect to calcite. Consequently, calcite dissolves at 295 atm and 82 °C until calcite saturation is re-established again, although ACF were saturated already with respect to calcite at 305 atm and 85 °C. This process will be continuously repeated as long as ACF migrate within the carbonate column following decreasing temperature and pressure. In summary, continuous calcite dissolution along the flow path of ACF is the inevitable consequence of the chemical–thermodynamic behaviour of the system 'ACF–calcite–$CO_{2(g)}$' while decreasing temperature and pressure – at least in the *P–T* range from 295 atm/82 °C to 205 atm/55 °C. Concurrent advective (dispersive and diffusive) mass transport controls the case-specific spatial and temporal distribution of calcite dissolution.

Such creation of porosity by ACF migration can be regarded as a spontaneous and self-propagating process. The total mass of calcite dissolved by ACF influx into the reservoir rock column (represented by the 1DRT modelling flow tube in this study) – in other words, the potential intensity of porosity creation – depends on the following factors: (1) the change in the temperature and pressure conditions along the ACF migration path; (2) the composition of the ACF influx already equilibrated with calcite; and (3) the duration of the ACF influx (corresponding to the 'number of pore volumes displaced' in the model). Starting from the assumption that the calcitic reservoir rock had an initial porosity of 10%, the creation of additional porosity can be recalculated from the amount of calcite dissolved during the time span that is equivalent to the 'number of pore volumes displaced (n)'. Porosity creation can be simply assessed by considering the 1DRT model scenario '11', a 'number of pore volumes displaced' ($n = 1000$) and the first of the 10 cells representing the migration path (Fig. 3). This recalculation of porosity creation is as follows: 1.0 l of pore is surrounded by 9.0 l of calcite (pre-assigned porosity of 10%), which is equivalent to 24.3 kg of calcite; 3.295 kg of calcite is lost by dissolution (Fig. 3). Assuming that the initial bulk rock volume remains constant without any compaction at 10.0 l (9.0 l + 1.0 l), a new pore volume of 2.22 l (1.0 l + 1.22 l, equivalent to 3.295 kg of calcite lost by dissolution) indicates that ACF migration into the reservoir rock caused an increase in reservoir porosity from initially 10% to finally 22% ($n = 1000$ which indicates how often the whole pore volume of the rock column has been displaced by the ACF influx). The 593 g of calcite dissolved within the last cell (scenario '11': $n = 1000$) (Fig. 3) is equivalent to an increase in reservoir porosity from initially 10% to finally 12%.

Taken into account that the duration of the ACF influx and also its acidity (pH and concentrations of $CO_{2(aq)}$ and CH_3COOH, which are controlled by the uptake of KMP) may range over several orders of magnitude, a broad porosity variability can be expected along the ACF *P–T* migration path (Fig. 4). It may start with a gain in porosity of less than 1% (e.g. from initially 10 to 11%) and end up locally with a structural breakdown of the calcite rock matrix, especially within zones exposed to preferential and long-lasting ACF flow. Consequently, a local compaction of the reservoir rock may also result from such ACF migration.

In parallel with calcite dissolution, the outgassing of $CH_{4(g)}$, $H_{2(g)}$ and $CO_{2(g)}$ in the form of a fixed-pressure multicomponent gas phase leads to the replacement of aqueous pore water by free gas bubbles. Their total volume may exceed the volume of the corresponding pore water, depending on: (1) the pressure–temperature conditions along the ACF migration path; (2) the composition of ACF influx already equilibrated with calcite; and (3) the duration of ACF influx ('number of pore volumes displaced' in the model). Such a displacement of aqueous solutions by gas bubbles provides a driving force for enhanced ACF migration.

ACF-induced calcite dissolution and outgassing result from the complex interplay of several factors driving the reactive transport system to calcite dissolution. Decreasing aqueous $CO_{2(aq)}$ solubility due to reduced pressure–temperature conditions along the ACF migration path leads to $CO_{2(g)}$ outgassing. Increasing solubility constants of calcite along the ACF pathway from higher to lower

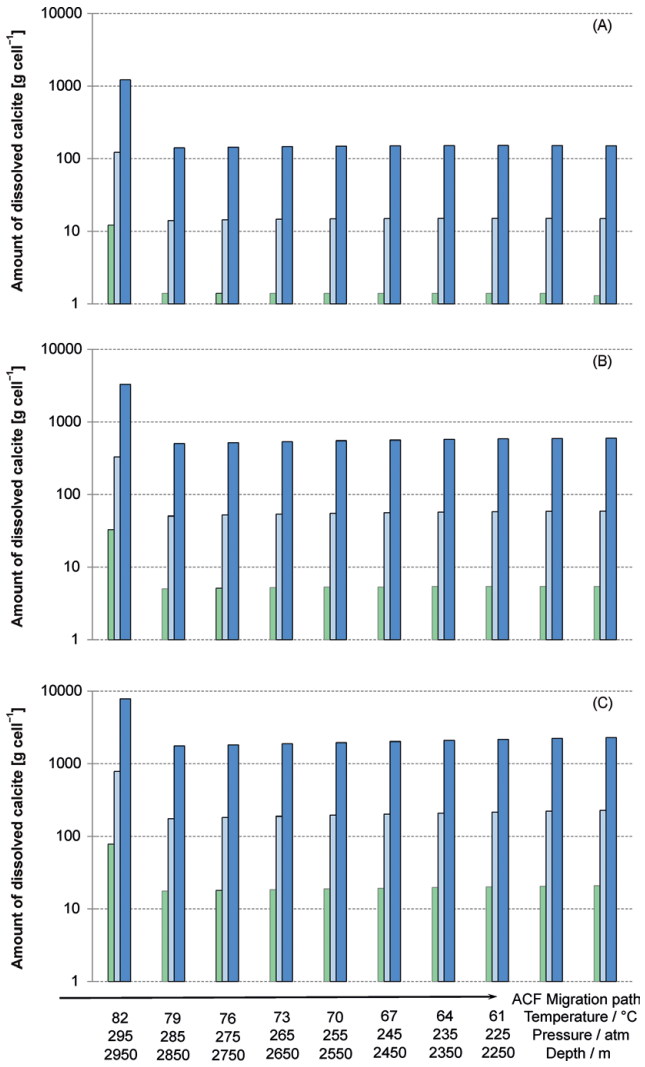

Fig. 4. Modelling results from 1DRT modelling scenarios (**a**) '10', (**b**) '11' and (**c**) '12'. Scenario '11' considers the average intensity of ACF generation by the release of 1.0 mol KMP (0.1 and 10.0 mol in scenarios '10' and '12', respectively). Amount of dissolved calcite (g cell^{-1}) along the migration path of ACF through the carbonate reservoir rock column for different 'numbers of pore volumes displaced (*n*)': green bars, $n = 10$; light-blue bars, $n = 100$: dark-blue bars: $n = 1000$.

temperature–pressure seem to (over-) compensate the effects of all other processes promoting calcite precipitation (e.g. $CO_{2(g)}$ outgassing). CO_2 outgassing itself is controlled by the combined and antagonistic effects of concurrent temperature and pressure decrease. On the one hand, decreasing pressure drives outgassing; on the other hand, a concurrent temperature decrease favours a higher aqueous $CO_{2(aq)}$ solubility and, thereby, reduces or even overcompensates pressure-driven outgassing. Within the complex web of inorganic interactions evolving during the reactive ACF transport, calcite solubility equilibration depends on many other reactions and on their specific temperature–pressure dependence (e.g. all reactions involving H^+ ions and controlling pH: all reactions involving complex Ca^{2+}, CO_3^{2-}, HCO_3^- and Cl^- species).

The key factor leading to the modelled dissolution of calcite along the modelled *P–T* migration path is of thermodynamic nature; this is a result of the pressure and temperature dependence of the thermodynamic equilibrium constants, K^a, of mass-action laws involved in all interacting equilibrium reactions. Such thermodynamic constants are, in general and per definition, independent of kinetic effects. Thus, such kinetic effects are basically incapable of influencing the thermodynamically controls of calcite dissolution by ACF migration. Nevertheless, kinetics may affect the temporal and spatial evolution of calcite dissolution along the modelled *P–T* migration path. Owing to the 'purely advective character' of our 1DRT modelling approach, it ignores any explicit definition of spatial (e.g. cell length) and temporal attributes (e.g. time step length, flow velocity).

Calcite dissolution along *P–T* migration paths of fluids may be triggered by all types of CO_2-bearing fluids, independent on the source of CO_2 – whether released by kerogen maturation or injected for storage.

Conclusions

The development of porosity creation in carbonate reservoir rocks due to the migration of pre-oil-phase corrosive fluids is a matter of debate in the geoscientific literature. Based on convincing evidence, Lambert *et al*. (2006) suggested that burial dissolution has enhanced microporosity in micritic Middle Eastern carbonate reservoirs by the influx of mixed (water–oil) corrosive fluids immediately before or during oil migration. In contrast, Ehrenberg *et al*. (2012, p. 224) pointed out that 'this process is implausible, however, because any excess acidity transported in the water phase would be neutralized by reaction in the conduit long before arriving in the reservoir and would in any case cause dissolution throughout the entire column height instead of only near the crest'.

The '0D' batch modelling results of ACF generation (ACF: acidic, corrosive and aqueous oil-/gas-bearing fluids) lead to the conclusion that a sufficient mass conversion of kerogen maturation can provide amounts of the thereby generated CO_2, CH_4, H_2 and CH_3COOH sufficient to cause the total consumption of the acid-neutralization capacity of the siliciclastic source rocks. This acid-neutralization capacity could be provided, for instance, by minor amounts of calcite, anorthite, albite and K-feldspar. The resulting ACF are characterized by a pH ranging from around 5 to 3, and may also contain high concentrations of dissolved $CO_{2(aq)}$ and acetic $acid_{(aq)}$. These calcite-corrosive ACF co-exist with a strongly altered mineral assemblage dominated by primary and newly formed quartz plus kaolinite, as well as by a methane- and carbon-dioxide-dominated gas.

The results of our hydrogeochemical modelling approach prove that the migration of such ACF can trigger continuous calcite dissolution and cause corresponding porosity creation along the migration path following decreasing temperature and pressure. Calculations of calcite solubility reveal an increase in calcite solubility in the system 'ACF–calcite–$CO_{2(g)}$' with decreasing temperature and pressure. This results from the pressure and temperature dependence of equilibrium constants, K^a, of mass-action laws involved in all interacting equilibrium reactions. The results of our one-dimensional reactive transport (1DRT) modelling of ACF migration through carbonate rock columns demonstrate the reasons and mechanisms of such calcite dissolution. Thermodynamically controlled chemical re-equilibration between ACF, calcite and $CO_{2(g)}$ along a migration path characterized by continuously decreasing pressure and temperature conditions is the driving force for continuous calcite dissolution. During their migration, ACF may saturate with respect to calcite ($SI_{calcite} = 0$: e.g. at 305 atm and 85 °C) before they reach the carbonate reservoir or at the direct entry point into the reservoir. Although saturated with respect to calcite (at 305 atm and 85 °C), a further migration of such ACF into and/or through the reservoir into areas characterized by lower pressure and temperature (e.g., 295 atm and 82 °C; within the reservoir) causes undersaturation of ACF with respect to calcite ($SI_{calcite} < 0$). Consequently, such migrating ACF dissolve calcite until the saturation is re-established (at 295 atm and 82 °C). During further ACF migration under lower pressure and temperature conditions (lower than 295 atm and 82 °C), this process of

repeated chemical re-equilibration with calcite evolves continuously. This reflects the increasing solubility of calcite in the system 'ACF–calcite–$CO_{2(g)}$' with decreasing pressure–temperature. In consequence, ACF can preserve their calcite-corrosive character along their migration path (e.g. from 295 atm/82 °C to 205 atm/55 °C). Continuous calcite dissolution along the flow path of ACF is the inevitable consequence of the chemical–thermodynamic behaviour of the system 'ACF–calcite–$CO_{2(g)}$' exposed to decreasing pressure–temperature – at least in the *P–T* range from 295 atm/82 °C to 205 atm/55 °C.

Porosity creation along the ACF migration path is not uniform: it causes highly variable porosities (Dunham & Larter 1981). Controls for this variability are the duration and the acidity of the ACF influx, which is controlled by the intensity of in-source rock kerogen maturation. The pressure and temperature regime is an additional factor. Such processes may start with a gain in porosity of less than 1% and end up with a local structural breakdown of the calcite rock matrix.

Therefore, we conclude that the above-described reasons and mechanisms of continuous in-reservoir calcite dissolution – the continuous and thermodynamically controlled re-equilibration at decreasing pressure–temperature – provide a plausible explanation for some observations made by Melville *et al*. (2004) and Lambert *et al*. (2006) regarding porosity creation in carbonate reservoirs of the Middle East. Such a reactive mass transport process should have its greatest impact in geological settings: (1) where ACF migration is at 'direct source rock–reservoir rock contacts' (wording after Beglinger *et al*. 2012); and (2) where relatively low acid buffering capacities of source rocks prevail – preferentially in siliciclastic instead of carbonate source rocks. Nevertheless, such settings with 'direct siliciclastic source rock–reservoir rock contacts' may provide preferred conditions for porosity creation, but are not a fundamental requirement.

Our modelling results are not in contradiction (in general) to the alternative explanation from Ehrenberg *et al*. (2012; pp. 225 and 226) regarding porosity creation in reservoir rocks. The authors suggested that oil charging the reservoir was the carrier for entrained, dissolved acidic components, which were subsequently released to the residual water in the oil column. In such a case, acidic components of the migrating oil must have caused a flux of total acidity similar to the total flux of acidity resulting from the ACF. In other words, a multifold displacement of pore water and oil by the influx of 'new and corrosive oil' is a prerequisite for such a mechanism of porosity creation.

In summary, organic–inorganic interactions driven by kerogen maturation and subsequent oil degradation in siliciclastic source rocks lead to: (1) ACF generation; and (2) subsequently to continuous calcite dissolution in carbonate reservoirs. These processes are the inevitable consequences of chemical thermodynamics of such systems at elevated temperature and pressure conditions. The involved hydrogeochemical reactions cause a geochemical environment that approaches to, and tends to reach, (metastable) equilibrium conditions (Helgeson *et al*. 1993).

Based on the thermodynamics of chemical equilibrium, hydrogeochemical modelling approaches can help to better identify and quantify diagenetic processes that are relevant for exploration and appraisal of hydrocarbon resources. The presented modelling approach contributes to support 'the theory that dissolution by acid pore water has produced significant net increases in bulk porosity' (Ehrenberg *et al*. 2012; p. 227) and follows their suggestion that 'diagenetic reactions must be constrained geochemically'.

However, the modelling results and conclusions may be transferred to optimize the reservoir engineering of CO_2 storage into carbonate rocks as calcite dissolves during the migration of aqueous CO_2-bearing solutions along gradients of decreasing pressure and temperature.

Acknowledgements and Funding

Without the groundbreaking work of D.L. Parkhurst (United States Geological Survey; Water Resources Investigations), who is continuously developing the PHREEQC modelling tool, our own work – like many other hydrogeochemical modelling papers – would not contribute to reveal the complexity of hydrogeochemical processes. We thank Ch. Hemme for reviewing the manuscript. We thank two anonymous reviewers for their valuable comments that helped to improve the manuscript.

References

Barth, T. & Bjørlykke, K. 1993. Organic acids from source rock maturation: Generation potentials, transport mechanisms and relevance for mineral diagenesis. *Applied Geochemistry*, **8**, 325–337.

Beglinger, S.E., Doust, H. & Cloetingh, S. 2012. Relating petroleum system and play development to basin evolution: Brazilian South Atlantic margin. *Petroleum Geoscience*, **18**, 315–336. http://dx.doi.org/10.1144/1354-079311-022.

Berkowitz, B. 2002. Characterizing flow and transport in fractured geological media: A review. *Advances in Water Resources*, **25**, 861–884.

Dunham, J.B. & Larter, S. 1981. Association of stylolitic carbonates and organic matter: Implications for temperature control on stylolite formation. *American Association of Petroleum Geologists Bulletin*, **65**, 922

Ehrenberg, S.N. & Jakobsen, K.G. 2001. Plagioclase dissolution related to biodegradation of oil in Brent Group sandstones (Middle Jurassic) of Gullfaks Field, northern North Sea. *Sedimentology*, **48**, 703–721, http://dx.doi.org/10.1046/j.1365-3091.2001.00387.x.

Ehrenberg, S.N., Walderhaug, O. & Bjørlykke, K. 2012. Carbonate porosity creation by mesogenetic dissolution: Reality or illusion? *American Association of Petroleum Geologists-Bulletin*, **96**, 217–233, http://dx.doi.org/10.1306/05031110187.

Helgeson, H.C., Knox, A.M., Owens, C.E. & Shock, E.L. 1993. Petroleum, oil field waters, and authigenic mineral assemblages: Are they in metastable equilibrium in hydrocarbon reservoirs? *Geochimica et Cosmochimica Acta*, **57**, 3295–3339, http://dx.doi.org/10.1016/0016-7037(93)90541-4.

Helgeson, H.C., Richard, L., McKenzie, W.F. & Norton, D.L. 1999. Thermodynamic constraints on the generation and maturation of petroleum in sedimentary basins. https://web.anl.gov/PCS/acsfuel/preprint%20archive/Files/44_2_ANAHEIM_03-99_0415.pdf.

Helgeson, H.C., Richard, L., McKenzie, W.F., Norton, D.L. & Schmitt, A. 2009. A chemical and thermodynamic model of oil generation in hydrocarbon source rocks. *Geochimica et Cosmochimica Acta*, **73**, 594–695, http://dx.doi.org/10.1016/j.gca.2008.03.00.

Lambert, L., Durlet, Ch., Loreau, J.-P. & Marnier, G. 2006. Burial dissolution of micrite in Middle East carbonate reservoirs (Jurassic–Cretaceous): Keys for recognition and timing. *Marine and Petroleum Geology*, **23**, 79–92, http://dx.doi.org/10.1016/marpetgo.2005.04.003.

Melville, P., Al Jeelani, O., Al Menhali, S. & Grötsch, J. 2004. Three-dimensional seismic analysis in the characterization of a giant carbonate field, onshore Abu Dhabi, United Arab Emirates. *In*: Eberli, G.P., Massaferro, J.L. & Sarg, R.F. (eds) *Seismic Imaging of Carbonate Reservoirs and Systems*. American Association of Petroleum Geologists, Memoirs, **81**, 123–148.

Parkhurst, D.L. & Appelo, C.A.J. 2013. *Description of Input and Examples for PHREEQC Version 3 – A Computer Program for Speciation, Batch-Reaction, One-Dimensional Transport, and Inverse Geochemical Calculations*. United States Geological Survey, Techniques and Methods, **6**, chap. **A43**, http://pubs.usgs.gov/tm/06/a43.

Pokrovskii, V.A. & Helgeson, H.C. 1994. Solubility of petroleum in oil-field waters as a fuction of the oxidation state of the system. *Geology*, **22**, 851–854, http://dx.doi.org/10.1130/0091-7613(1994)0222.3.CO;2.

Seewald, J.S. 2003. Organic–inorganic interactions in petroleum-producing sedimentary basins. *Nature*, **426**, 327–333, http://dx.doi.org/10.1016/marpetgo.2005.04.003.

Smith, J.T. & Ehrenberg, S.N. 1989. Correlation of carbon dioxide abundance with temperature in clastic hydrocarbon reservoirs: Relationship to inorganic chemical equilibrium. *Marine and Petroleum Geology*, **6**, 129–135, http://dx.doi.org/10.1016/0264-8172(89)90016-0.

van Berk, W., Schulz, H.-M. & Fu, Y. 2009. Hydrogeochemical modelling of CO2 equilibria and mass transfer induced by organic–inorganic interactions in siliciclastic petroleum reservoirs. *Geofluids*, **9**, 253–262. http://dx.doi.org/10.1111/j.1468-8123.2009.00256.x.

van Berk, W., Schulz, H.-M. & Fu, Y. 2013. Controls on CO2 fate and behavior in the Gullfaks oilfield (Norway): How hydrogeochemical modeling can help to decipher organic-inorganic interactions. *American Association of Petroleum Geologists-Bulletin*, **97**, 2233–2255, http://dx.doi.org/10.1111/j.1468-8123.2009.00256.x.